Title

Exacerbated brain edema in a rat streptozotocin model of hyperglycemic ischemic stroke: Evidence for involvement of blood–brain barrier Na–K–Cl cotransport and Na/H exchange

Journal

Cerebrovascular and Brain Metabolism Reviews, 39(9)

ISSN

1040-8827

Authors

Yuen, Natalie Y
Chechneva, Olga V
Chen, Yi-Je
et al.

Publication Date

2019-09-01

DOI

10.1177/0271678x18770844

Peer reviewed

Original Article

JCBFM

Journal of Cerebral Blood Flow & Metabolism
2019, Vol. 39(9) 1678–1692

DOI: 10.1177/0271678X18770844
journals.sagepub.com/home/jcbfm
SAGE

Exacerbated brain edema in a rat streptozotocin model of hyperglycemic ischemic stroke: Evidence for involvement of blood–brain barrier Na–K–Cl cotransport and Na/H exchange

Natalie Y Yuen[1], Olga V Chechneva[1], Yi-Je Chen[2], Yi-Chen Tsai[1], Logan K Little[1], James Dang[1], Daniel J Tancredi[3], Jacob Conston[1], Steven E Anderson[1] and Martha E O'Donnell[1]

Abstract

Cerebral edema is exacerbated in diabetic ischemic stroke through poorly understood mechanisms. We showed previously that blood–brain barrier (BBB) Na–K–Cl cotransport (NKCC) and Na/H exchange (NHE) are major contributors to edema formation in normoglycemic ischemic stroke. Here, we investigated whether hyperglycemia-exacerbated edema involves changes in BBB NKCC and NHE expression and/or activity and whether inhibition of NKCC or NHE effectively reduces edema and injury in a type I diabetic model of hyperglycemic stroke. Cerebral microvascular endothelial cell (CMEC) NKCC and NHE abundances and activities were determined by Western blot, radioisotopic flux and microspectrofluorometric methods. Cerebral edema and Na in rats subjected to middle cerebral artery occlusion (MCAO) were assessed by nuclear magnetic resonance methods. Hyperglycemia exposures of 1-7d significantly increased CMEC NKCC and NHE abundance and activity. Subsequent exposure to ischemic factors caused more robust increases in NKCC and NHE activities than in normoglycemic CMEC. MCAO-induced edema and brain Na uptake were greater in hyperglycemic rats. Intravenous bumetanide and HOE-642 significantly attenuated edema, brain Na uptake and ischemic injury. Our findings provide evidence that BBB NKCC and NHE contribute to increased edema in hyperglycemic stroke, suggesting that these Na transporters are promising therapeutic targets for reducing damage in diabetic stroke.

Keywords

Blood–brain barrier, brain edema, cerebral ischemia, hyperglycemia, sodium transporters

Received 19 December 2016; Revised 20 March 2018; Accepted 20 March 2018

Introduction

Cerebral edema is a leading cause of morbidity and mortality in stroke. During the early hours of ischemic stroke, edema develops by mechanisms involving increased transendothelial secretion of Na, Cl and water from blood into brain across an intact blood–brain barrier (BBB).[1–4] Our previous studies have shown that the BBB Na–K–Cl cotransporter (NKCC) and Na/H exchanger (NHE) are major participants in ischemia-induced cerebral edema formation. Both NKCC and NHE are present in the luminal BBB membrane and are stimulated by hypoxia, aglycemia and

[1]Department of Physiology and Membrane Biology, University of California, Davis, CA, USA
[2]Department of Pharmacology, University of California, Davis, CA, USA
[3]Department of Pediatrics, University of California, Davis, CA, USA

The first two authors contributed equally to this work.

Corresponding author:
Martha E O'Donnell, Department of Physiology and Membrane Biology, School of Medicine, University of California, One Shields Ave., Davis, CA 95616, USA.
Email: meodonnell@ucdavis.edu

arginine vasopressin (AVP), three prominent factors present during cerebral ischemia.[1,2,5–10] Further, inhibition of BBB NKCC and/or NHE by intravenous administration of bumetanide and/or HOE-642 significantly reduces edema, brain Na uptake and injury, as well as improves neurological outcome in the rat middle cerebral artery occlusion (MCAO) model of stroke.[1,2] While this is a promising approach to reduce edema formation during ischemia in otherwise healthy individuals, a major fraction of ischemic stroke patients have co-morbidities present at the time of stroke. Diabetes, the most rapidly increasing risk factor for stroke, is associated with greatly increased post-stroke mortality,[11,12] and hyperglycemia, independent of diabetes, worsens stroke outcome.[11–15] Whether hyperglycemic patients have type I or type II diabetes or other causes of hyperglycemia, the consistent finding is that they have more robust edema, greater injury and worse neurological outcome.[11,12,16] However, the reasons for this are not well understood. Studies have shown that hyperglycemia can alter expression and/or activity of NKCC and NHE in a variety of tissues. High glucose increases activity of NHE in vascular smooth muscle cells[17] and both expression and activity in glomerular mesangial cells,[18] while rats with streptozotocin (STZ)-induced diabetes have increased NKCC activity in aorta and choroid plexus.[19,20] Given that BBB NKCC and NHE play prominent roles in ischemia-induced cerebral edema and that hyperglycemia exacerbates edema formation in stroke, we hypothesized that the detrimental effects of hyperglycemia in stroke involve increased expression and activity of BBB NKCC and/or NHE and consequently, more robust ischemia-induced edema formation.

In the present study, we evaluated the effects of hyperglycemia on cerebral microvascular endothelial cell (CMEC) NKCC and NHE expression and activity, as well the effects of ischemic factors on these Na transporter activities in CMEC subjected to hyperglycemic versus normoglycemic conditions. Using magnetic resonance methods, we also evaluated the magnitude of MCAO-induced brain edema and brain Na uptake in rats with pronounced hyperglycemia compared to normoglycemic rats. Our goal in these studies was to investigate the effects of hyperglycemia on processes underlying ischemia-induced cerebral edema. Hyperglycemic stroke patients can be either type I and type II diabetics, although type II is more common, with hyperinsulinemia generally accompanying hyperglycemia. Because insulin can stimulate NKCC or NHE activity in some cell types[21–23] in the present study, we evaluated hyperglycemia in the absence of insulin, using the STZ model of hyperglycemia. Although this model more closely mimics type I than type II diabetes, it allows us to investigate the effects of hyperglycemia without possible added effects of insulin.

Finally, we tested whether administering intravenous bumetanide and HOE-642 to inhibit BBB NKCC and NHE activities, respectively, effectively reduces brain edema and brain Na uptake in hyperglycemic rats subjected to MCAO as we demonstrated previously in normoglycemic rats. Our studies provide evidence that exposing CMEC to hyperglycemia does indeed significantly increase abundance and activity of CMEC NKCC and NHE, "priming" the system such that subsequent exposure to ischemic factors results in significantly greater NKCC and NHE activities than observed in normoglycemic cells. Our studies also provide evidence that both bumetanide and HOE-642 significantly reduce edema, brain Na uptake and injury following MCAO in the hyperglycemic rats. Our findings support the hypothesis that BBB NKCC and NHE are promising therapeutic targets for reduction of edema and injury in a type 1 diabetes model of hyperglycemic stroke as well as normoglycemic stroke.

Materials and methods

CMEC culture

Bovine CMECs (Cell Systems, Kirkland, WA) were grown on collagen- and attachment factor- (Cell Systems, Kirkland, WA) coated multiwell plates or cover slips in DMEM supplemented with 2 mM L-glutamine, 50 μg/ml gentamicin (AG Scientific), 1 ng/ml basic fibroblast growth factor, 5% calf serum and 5% horse serum at 37°C in a humidified atmosphere of 95% air-5% CO_2. Cells were refed fresh growth medium every 48 h until reaching confluence, then the medium was replaced with DMEM-astrocyte-conditioned medium (DMEM-ACM, 1:1 by volume).[24] For experimental treatments, cells were exposed to DMEM-ACM containing 5 mM D-glucose (control, 298 mOsm) or to DMEM:ACM with added 25 mM D-glucose (hyperglycemia, 323 mOsm), 25 mM mannitol (mannitol osmotic control) or 12.5 mM NaCl (NaCl osmotic control) for 6, 24 or 48 h or seven days. For these initial investigations of hyperglycemia effects on BBB ion transporters, we used 30 mM glucose because it mimics the level of pronounced hyperglycemia observed in our rat STZ model of diabetes. During seven-day treatments, cells were refed every 48 h with the appropriate experimental condition DMEM-ACM medium.

Western blot analysis

Cell lysates for Western blot analysis were prepared by rinsing CMEC grown on 24 well plates with

ice-cold PBS and lysing with RIPA buffer containing protease inhibitors (cOmplete Protease Inhibitor Cocktail, Roche Diagnostic, Indianapolis, IN). Lysate proteins were then denatured in SDS buffer containing 50 mM DTT (Invitrogen NuPage, Carlsbad) and heated for 10 min at 70°C. Proteins (10 μg/lane) and prestained molecular weight makers were separated on 7.5% Tris-HCl gels (Lonza PAGEr Gold Precast Gel; Rockland) and transferred to PVDF or nitrocellulose membranes (BioRad, Hercules, CA). Membranes were blocked using 7.5% milk in PBS with 0.1% Tween-20 (PBST) for 1 h at room temperature and incubated overnight at 4°C with mouse anti-NHE1 (1:2000, Millipore), rabbit anti-NHE2 (1:1000, Millipore), mouse anti-NKCC1 (1:2000, University of Iowa Hybridoma Bank. Iowa City, IA) or mouse anti-β-actin (1:75000, Abcam, Cambridge, MA). Membranes were washed with PBST and incubated with respective secondary antibody: HRP-conjugated goat anti-mouse or anti-rabbit IgG (1:2000, Zymed Laboratories, South San Francisco, CA) for PVDF membranes, and IRDye 800CW goat anti-mouse or IRDye 680RD goat anti-rabbit IgG (Li-Cor, Lincoln NE) for nitrocellulose membranes for 1 h at room temperature. After washing, PVDF membranes were developed using enhanced chemiluminescence substrate (GE Healthcare, Buckinghamshire, UK) and visualized on a Fuji Film LAS-4000 Imaging Machine (Medford, UK). Proteins on nitrocellulose membranes were visualized using Odyssey Infrared Imager (Li-Cor). MultiGuage software (Science Lab 2005, Fuji Film) or ImageJ (NIH) was used to quantify band density. Protein abundance was normalized to β-actin.

RNA isolation and qPCR

Total RNA was isolated from CMEC using RNAse Mini Kit following the standard protocol (Qiagen, Germantown, MD). For quality control, RNA purity was verified by the OD260/280 ratio falling between 1.8 and 2.0. Total RNA (1 μg) was reverse-transcribed to cDNA using MultiscribeTM reverse transcriptase (Applied Biosystems, Foster City, CA). Subsequent qPCR reactions for β-actin, NKCC1 and NHE1 were performed in triplicate on a Roche Light Cycler 480 using SYBR Green Master Mix (Roche Applied Science, Indianapolis, IN). Specific primers were designed using Primer3 Input software. Primers used were: β-actin forward: 5′-CTCTTCCAGCCTTCCTT CCT-3′; β-actin reverse: 5′-TAGAGGTCCTTGCGG ATGTC-3′; NKCC1 forward: 5′-GGCCACTGTCG TGACAACTA-3′; NKCC1 reverse: 5′-TGGCAAAA GCGAAGATCAG-3′; NHE1 forward: 5′-CATCCTT GTGTTTGGGGAGT-3′; NHE1 reverse: 5′-ACCACG AAGAAGCTCAGGAA-3. The specificity of products from each primer set was validated by melting curve (Tm) analysis. All experimental samples were normalized to the expression level of the internal control gene, β-actin. Relative quantification of fold-change was performed by applying the $2^{-\Delta\Delta Ct}$ method and comparing Cp values (calculated by second derivative maximum) of treated groups to control group.[25]

NKCC cotransporter activity assay

NKCC activity of CMEC monolayers grown on 24-well plates and pre-exposed to normoglycemic or hyperglycemic media was evaluated as ouabain-insensitive, bumetanide-sensitive K flux, using ^{86}Rb as a tracer for K as described by us previously.[5,26] Cells were placed in a hypoxia chamber with desired O_2 levels (19 or 2% O_2). Growth medium was immediately replaced with normoxic or hypoxic HEPES-DMEM pretreatment medium comprising (in mM) 110 NaCl, 5.3 KCl, 0.81 $MgSO_4$, 1.8 $CaCl_2$, 0.9 NaH_2PO_4, 44 $NaHCO_3$, 1.0 Na-pyruvate and 10 mM HEPES at pH 7.45 plus 5.5 or 30 mM D-glucose. For osmotic control media, 12.5 mM NaCl or 25 mM mannitol was added to the HEPES DMEM 5.5 mM glucose medium. In some experiments, the media also contained AVP (100 nM). For aglycemia experiments, glucose and pyruvate were replaced with NaCl to maintain osmolality. Cells were incubated in the appropriate pretreatment medium at 37°C for 60 min, with bumetanide (10 μM, INC Biomedicals) and/or ouabain (100 μM, INC Biomedicals, Costa Mesa, CA) present during the last 5 min. Cells were then incubated for 5 min in assay media identical to pretreatment media but containing 0.25 μCi/ml ^{86}Rb (Perkin-Elmer, Welles, MA). The assay was terminated by washing cells with ice-cold 0.1 M $MgCl_2$. Cell-associated radioactivity was determined by liquid scintillation counting after extraction in 2% SDS. Protein per well was determined by BCA assay (Pierce, Rockford, IL). K flux data are presented as μmol K/gm protein/min.

NHE activity assay

CMEC NHE activity was determined as Na-dependent, HOE-642-sensitive H flux using the pH sensitive dye BCECF and the well-established NH_4 prepulse method.[6] Cells grown on coverslips and exposed to experimental conditions as described for NKCC activity were incubated for 60 min at 37°C in normoxic or hypoxic HEPES-buffered pretreatment media. BCECF-AM (5 μM) was added during the last 20 min. Coverslips were then placed in a closed, temperature controlled perfusion-imaging chamber (Warner Instrument, Hamden) and mounted on the stage of an Axiovert inverted microscope (Carl Zeiss, Germany). Cells were

superfused at 37°C with pretreatment media for 5 min at 2 ml/min to wash out extracellular BCECF and measure baseline F490/F440 fluorescence, then superfused with 20 mM NH_4Cl in HEPES medium and then Na-free HEPES medium for 5 min each. This was followed by superfusion with HEPES medium (containing Na) with 25 μM HOE-642 (gift from Sanofi-Aventis Pharmaceuticals, Bridgewater, NJ) for 5 min and then finally with HEPES medium without HOE-642. NHE activity was determined from the maximum rate of pHi recovery and is expressed as Na-dependent HOE-642-sensitive H^+ flux in mM/min, calculated as the product of ΔpH_i/min and buffer capacity (β) at the corresponding pH_i. pHi was calculated from the ratios of fluorescence intensities at excitation wavelengths of 490 and 440 nm and emission at 535 nm (F490/F440) as described previously.[6]

Induction of hyperglycemia in rats

Animal studies were approved by the University of California, Davis, Animal Use and Care Committee and conducted in accordance with the United States Public Health Service Policy on the Humane Care and Use of Laboratory Animals and the Guide for the Care and Use of Laboratory Animals. Animal care was in accord with the National Institutes of Health Guidelines and ensured animal comfort. The study was conducted in compliance with all ARRIVE guidelines. Male Sprague-Dawley rats (six-to-eight weeks old, 200–250 g, Charles River Laboratories, Wilmington, MA) were housed two per cage in standard cages and were acclimatized to the vivarium for five to seven days. For induction of hyperglycemia, rats were administered STZ (90 mg/kg) or vehicle intraperitoneally as described previously[27] and then after 24 h rats were treated with subcutaneous insulin (Novolin 70/30 insulin, 5 units daily) for five to seven days to normalize blood glucose. Urine glucose and ketoacid (acetoacetate) were tested daily by Keto-Diastix urinalysis strips (Bayer, Whippany, NJ). Rats with abnormal urine acetoacetate levels (>0.5 mmol/L) were excluded from experimental groups (12% of rats in this study). Insulin treatment was stopped 48 h prior to focal ischemia studies to allow development of hyperglycemia. While other models of diabetes are available, the STZ model was chosen for this study because it allows investigation of hyperglycemia effects in absence of insulin. This is important because insulin has been shown to regulate activity of ion transporters in various cells.[21,22,28–30]

Induction of focal cerebral ischemia

Rats were subjected to permanent middle cerebral artery occlusion (pMCAO) by the intraluminal suture method as previously described.[1,2] For this, rats were anesthetized by using box induction with isoflurane (5%) in medical grade oxygen and then maintained on 0.5 to 1.5% isoflurane via a facemask. The left femoral artery and vein were cannulated with PE-50 polyethylene tubing. The left common carotid artery (CCA) was exposed and then occipital and thyroid artery branches of the external carotid artery (ECA) and pterygopalatine artery of internal carotid artery (ICA) were ligated. The ECA was ligated distally from the CCA and a silicone rubber-coated nylon monofilament with a tip diameter of 0.43 ± 0.02 mm (Doccol Corp., CA) was inserted into the ECA and advanced to the origin of the middle cerebral artery (MCA). MCA occlusion with 70–80% cerebral blood flow (CBF) reduction was confirmed by Laser Doppler (Moor Instruments, DE). Rats with CBF reduction less than 70% were excluded from the study (17% of the rats in this study). Bumetanide (30 mg/kg, ICN Biomedicals, Costa Mesa, CA) or/and HOE-642 (15 mg/kg; gift from Sanofi-Aventis Pharmaceuticals, Bridgewater, NJ) were administered intravenously via the femoral vein cannula immediately before occlusion of the MCA. To eliminate any possible renal diuretic effect of the Na transport inhibitors, nephrectomy was performed immediately prior to MCAO surgery as described previously.[1,31] Body temperature was monitored throughout surgery and subsequent imaging by rectal probe and maintained at 36.8–37.0°C by electric heating pad (Cole-Parmer Instruments, IL) during surgery and water heating pad (Gaymar, NY) during imaging. Rats were also ventilated via tracheal intubation (Harvard Small Animal Ventilator, MA) during imaging. Blood samples were taken from the femoral artery cannula for pCO2 and pH measurements after ventilation. Respiratory rate and tidal volume were adjusted to maintain pCO2 level within the normal range.

Magnetic resonance diffusion-weighted imaging analysis of edema formation

MR diffusion-weighted imaging (DWI) was performed using a 7-T Bruker Biospec magnetic resonance spectroscopy/MRI system (Bruker, Billerica, MA) as described previously.[1,2] At the end of pMCAO surgery, rats were switched to sodium pentobarbital anesthesia for the remainder of the experiment (65 mg/kg i.p. initial dose) with maintenance doses given as needed by femoral catheter. Rats were positioned in a 72-mm radio frequency probe inside the 7-T magnet and diffusion-weighted spin echo images (2-mm slices) were acquired at 38 to 170 min following induction of pMCAO. Apparent diffusion coefficient (ADC) values (10^{-6} cm^2/s) from regions of interest (ROIs; Figure 3(a)) were determined using four gradient strengths and Paravision 2.1 software.

The ROIs were chosen to assess ADC values in three cortical regions and one striatal region in both ipsilateral and contralateral hemispheres. Placement of the four ROIs was done for each rat using anatomical landmarks for consistency.

Assessment of diffusion lesion volume

DWI images acquired for evaluation of edema formation were also used to assess the extent of ischemic injury in the rats subjected to pMCAO and treated with vehicle, bumetanide or HOE-642. Previous studies have shown that diffusion lesion volumes determined from DWI data are equivalent to ischemic injury volumes assessed by 2,3,5-Triphenyltetrazolium Chloride (TTC) staining methods at 24 h after the start of MCAO.[32,33] Here, we used the images from the final DWI scan (170 min) to manually outline the maximal visual extent of the B990 abnormality as previously described.[32] For each brain, the ischemic injury of a coronal section (7 mm from the frontal pole) was calculated as percent of the total ipsilateral hemisphere, corrected for brain swelling by previously described methods.[1]

Magnetic resonance chemical shift imaging of brain Na

Magnetic resonance chemical shift imaging (CSI) was used to determine changes in brain Na content of rats during MCAO as described previously.[2] Briefly, rats were positioned in the bore of the Bruker Biospec MRS/MRI system such that the head was centered in a double tuned 1H/23Na probe (Doty Scientific, Columbia, SC). Shimming was optimized using the 1H channel and scout images were acquired for locating Na CSI voxels. Two-dimensional Na CSI images of 4 mm thick slices were acquired in a 32×32 matrix with a FOX of 64 mm via the standard Bruker CSI protocol as described previously.[2] Acquisition time was 21 min for each 23Na CSI data set acquired over the course of the pMCAO experiment. Brain Na values presented in Figure 5 are those observed at the times shown from the start of occlusion. Data were Fourier transformed using MATLAB to generate a spectrum for each pixel corresponding to a 1 mm $\times$ 1 mm $\times$ 4 mm voxel, then spectra were further analyzed by MATLAB to integrate over the Na peak and that of an external Na standard to calculate brain [Na] using the following equation

$$[Na]_r = \left(S_r \times [Na]_s\right)/(\exp(-TE/T2_r) \times S_s)$$

where S is the integrated signal intensity measured for any voxel, TE is the delay between the excitation pulse and the beginning of data acquisition, and the subscripts r and s indicate rat brain and external standard, respectively.

Statistical analyses

Data were analyzed for significance using ANOVA with Tukey's or Bonferroni's multiple comparison tests as described in Figures 1 to 3 and 6. In vivo data of Figure 3 were also evaluated by repeated measures ANOVA. In all cases, p values less than 0.05 were considered statistically significant. Data of in vivo experiments presented in Figures 4 and 5 were evaluated in Stata Version 14 using mixed-effects regression models as described in Figure 4 and in Supplementary Information. No exclusions were made in in vitro experiments. For in vivo MCAO experiments, rats with occlusions less than 70% were excluded. This resulted in exclusion of seven rats (two, three and two in the vehicle, bumetanide and HOE-642 groups, respectively). For MCAO brain Na experiments, two normoglycemic rats were excluded and six hyperglycemic rats, two each from the vehicle and bumetanide groups. Western blot and NKCC assays were randomized by varying positions of conditions in the assay lanes/wells/coverslips. For MCAO studies, the order of experimental groups tested was randomized. These experiments were conducted independently by three individuals. For Figure 4 (ADC data), there were three surgeons; one (YJC) did five vehicle, five bumetanide and two HOE; a second (YCT) did five vehicle, five bumetanide and three HOE; a third (LKL) did three vehicle experiments. YJC trained and closely supervised the other two surgeons. For Figure 5 (Na data), there were two surgeons. YJC did 13 vehicle, 8 bumetanide and 5 HOE and LKL did 3 vehicle, 2 bumetanide and 5 HOE. All surgeries were all done in the same surgical suite using the same surgical, anesthesiology and monitoring instrumentation. A limitation of our study design is that no formal method of randomization was used in assigning rats to treatment groups. However, for each experiment, assignment of treatment as vehicle, bumetanide or HOE-642 was arbitrarily selected by the operator in a manner blinded to other operators. Individual investigators for both in vitro and in vivo experiments knew group allocations during experiments. Data analyses were performed both by those investigators and also separately by additional investigators to avoid bias. Prior to conducting our studies, we used G*Power 3 Statistical Analysis Software (Heinrich Heine University Düsseldorf) for ANOVA experiments, based on outcome-specific assumptions about within-group standard deviations and differences among means that would be important to detect. We powered the study to be able to detect

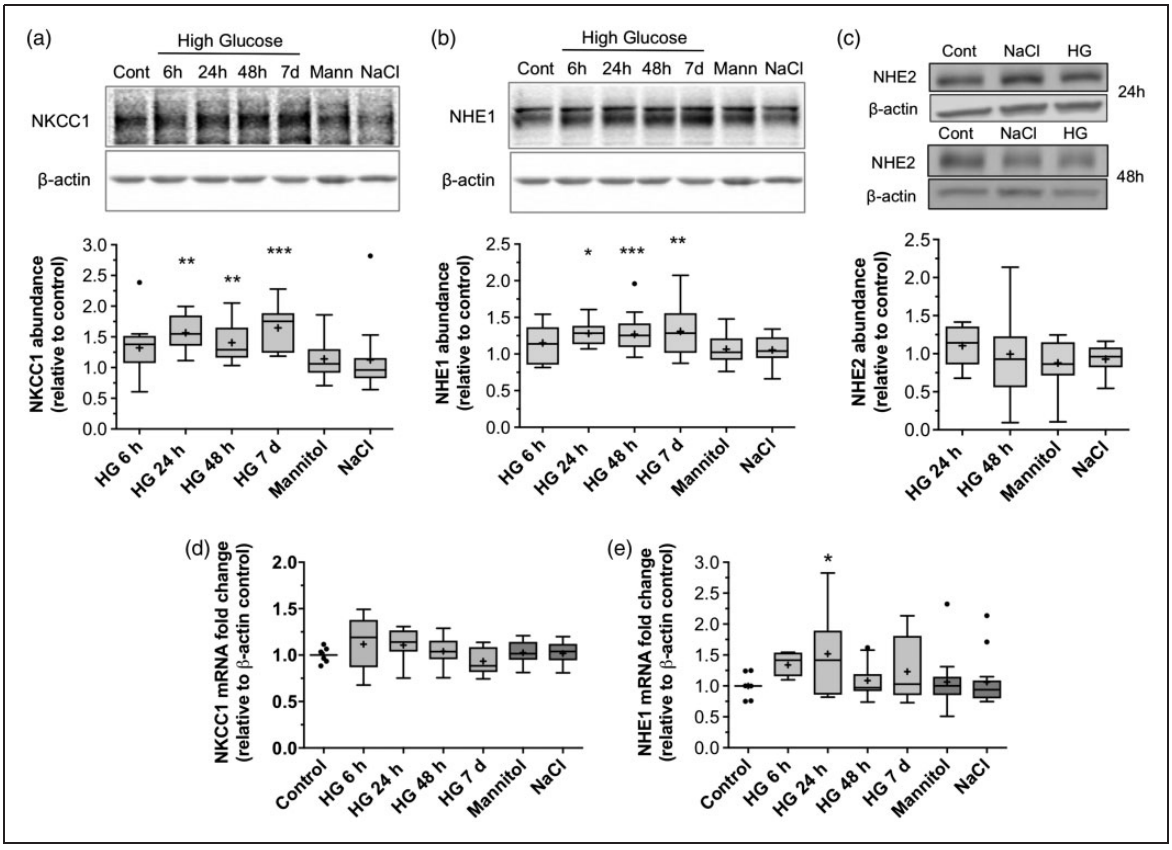

Figure 1. Hyperglycemia-induced increases in NKCC1 and NHE1 protein abundances. Cerebral microvascular endothelial cells (CMEC) were exposed for 6, 24 or 48 h or seven days to hyperglycemic medium or normoglycemic control media that were either isosmotic (298 mosm/L; Control) or hyperosmotic (323 mOsm/L) by addition of mannitol (Mann) or NaCl. Cell lysates were subjected to Western blot analysis using antibodies specific to NKCC1 or NHE1 as described in Methods. (a–c) Representative Western blots and densitometric quantitation of CMEC NKCC1, NHE1 and NHE2 protein abundances. Data are presented as Tukey box and whisker plots. Median values are shown as the horizontal line in the box. Mean values are indicated by the + sign. In (a), *n* values for 6, 24, 48 h and seven days HG exposures are 13, 8, 23 and 10, respectively, and for mannitol and NaCl, the *n* values are 18 and 12, respectively. In (b), *n* values for 6, 24, 48 h and seven days HG exposures are 14, 9, 25 and 12, respectively, and for mannitol and NaCl, the *n* values are 20 and 16, respectively. In (c), *n* values for 24 and 48 h HG and for mannitol and NaCl are 6, 10, 9 and 8, respectively. (d,e) NKCC1 and NHE1 mRNA levels in CMEC exposed to hyperglycemia. CMEC lysates were subjected to qRT-PCR as described in Methods. Data are presented as Tukey box and whisker plots. *Significantly different than control by ANOVA with Tukey's multiple comparison test, $p < 0.05$. In (d), *n* values for 6, 24, 48 h and 7 d HG exposures are 9, 7, 16 and 9, respectively, and for mannitol and NaCl, the *n* values are 13 each. In (e), *n* values for 6, 24, 48 h and seven days HG exposures are 7, 7, 17 and 7, respectively, and for mannitol and NaCl, the *n* values are 13 each. (a–e) asterisks indicate values significantly different than control by ANOVA with Tukey's multiple comparison test, *$p < 0.05$, **$p < .005$, ***$p < .0001$.

effect sizes that corresponded to approximately 20% point relative differences from the control group means, with two-sided a error probability of 0.05 and with a power of 0.8. Based on preliminary data, we assumed that the coefficient of variation in the control group was approximately 10% for Western blot evaluation of NKCC and NHE abundance measures and approximately 12% for the remaining outcomes, corresponding to standardized effect sizes of 2 and 1.67, respectively. Hence, the per-group target sample sizes were five for evaluation of NKCC and NHE abundances; seven for evaluation of NKCC and NHE activities; and seven for evaluation of edema and brain Na. Some of the original sample size targets were abandoned because the standard deviations were found to be different than assumed by the power analysis. All tests and confidence intervals are two-sided and because this was an exploratory study, we opted to use multiple comparison methods only within separate analyses, not for the entire family of hypotheses

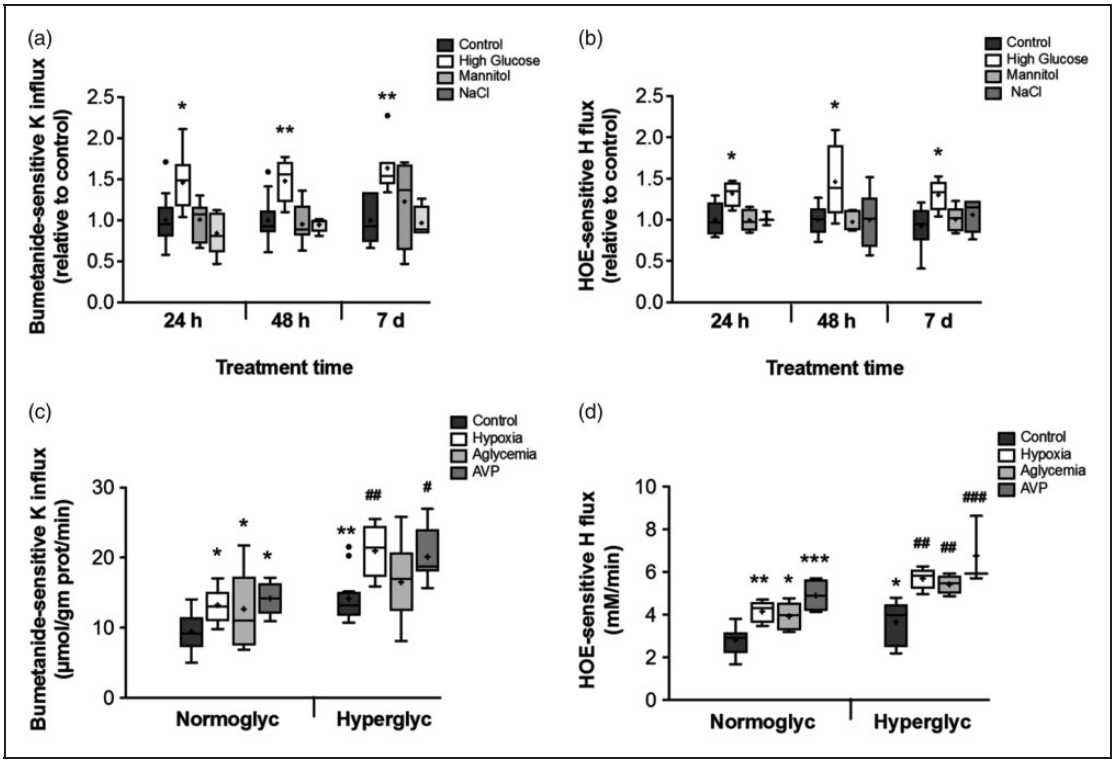

Figure 2. Hyperglycemia-induced increases in CMEC NKCC and NHE activities. (a,b) CMEC were exposed for 24 h, 48 h or seven days to hyperglycemic or normoglycemic media as described in Figure 1 for NKCC (a) and NHE (b) activities as described in Methods. Data are presented as Tukey box and whisker plots. Median values are shown as the horizontal line in the box. Mean values are indicated by the + sign. In (a), *n* values for control, high glucose, mannitol and NaCl are 16, 11, 11 and 15, respectively, for 24 h treatment time, 17, 10, 10 and 7 for 48 h treatment time and 7, 7, 4 and 4 for seven days treatment time. In (b), *n* values for control, high glucose, mannitol and NaCl are 13, 4, 5 and 3, respectively, for 24 h treatment time, 7, 12, 5 and 6 for 48 h treatment time and 12, 4, 5 and 5 for seven days treatment time. Asterisks indicate values significantly different than control by ANOVA with Tukey's multiple comparison test, $*p < 0.05$, $**p < .005$. (c,d) CMEC exposed to hyperglycemic or normoglycemic media for 48 h were subsequently exposed to normoxia (19% O_2), hypoxia (2% O_2), aglycemia or AVP (100 nM) for 60 min and then assessed for NKCC activity (c) or NHE activity (d) with pretreatment conditions maintained throughout the assay. Tukey box and whisker plots are as described for A–B. In (c), *n* values for control, hypoxia, aglycemia and AVP are 35, 9, 12 and 6, respectively, for normoglycemic media pre-exposure, and 12, 9, 15 and 8, respectively for hyperglycemic media pre-exposure. In (d), *n* values for control, hypoxia, aglycemia and AVP are 15, 5, 5 and 4, respectively for normoglycemic media pre-exposure, and 13, 5, 5 and 3, respectively for hyperglycemic media pre-exposure. *Significantly different than normoglycemic control by ANOVA with Tukey's multiple comparison test, $*p < 0.05$, $**p < .005$. #Significantly different than hyperglycemia by ANOVA with Tukey's multiple comparisons test, $\#p < 0.05$, $\#\#p < .005$, $\#\#\#p < .0001$.

evaluated in the paper. In this study, the terms ''increased'' or ''reduced'' are meant to indicate that values are higher (or lower) than one group compared to another.

Results

Hyperglycemia increases NKCC and NHE protein abundance and activity in BBB endothelial cells

To determine whether hyperglycemia exacerbation of ischemia-induced edema formation involves changes in BBB NKCC and/or NHE, we first evaluated the effects of exposing cultured CMECs to high glucose media over 6 h to seven days. Western blot analysis showed that both NKCC1 and NHE1 protein abundances were significantly increased after 24 h, 48 h and seven days of high glucose (increases of 57%, 41% and 65%, respectively, for NKCC1 and 28%, 27% and 31%, respectively for NHE1; Figure 1(a) and (b)). Six-hour exposures showed a trend for increased protein that did not reach statistical significance. Because the high glucose media have increased osmolarity (323 mosm/L versus 298 mosm/L Control), we also tested the effects of 323 mosm/L media prepared by addition of mannitol (25 mmol/L) or NaCl (12.5 mmol/L) instead of glucose. Neither of these osmotic controls altered abundance of NKCC1 or

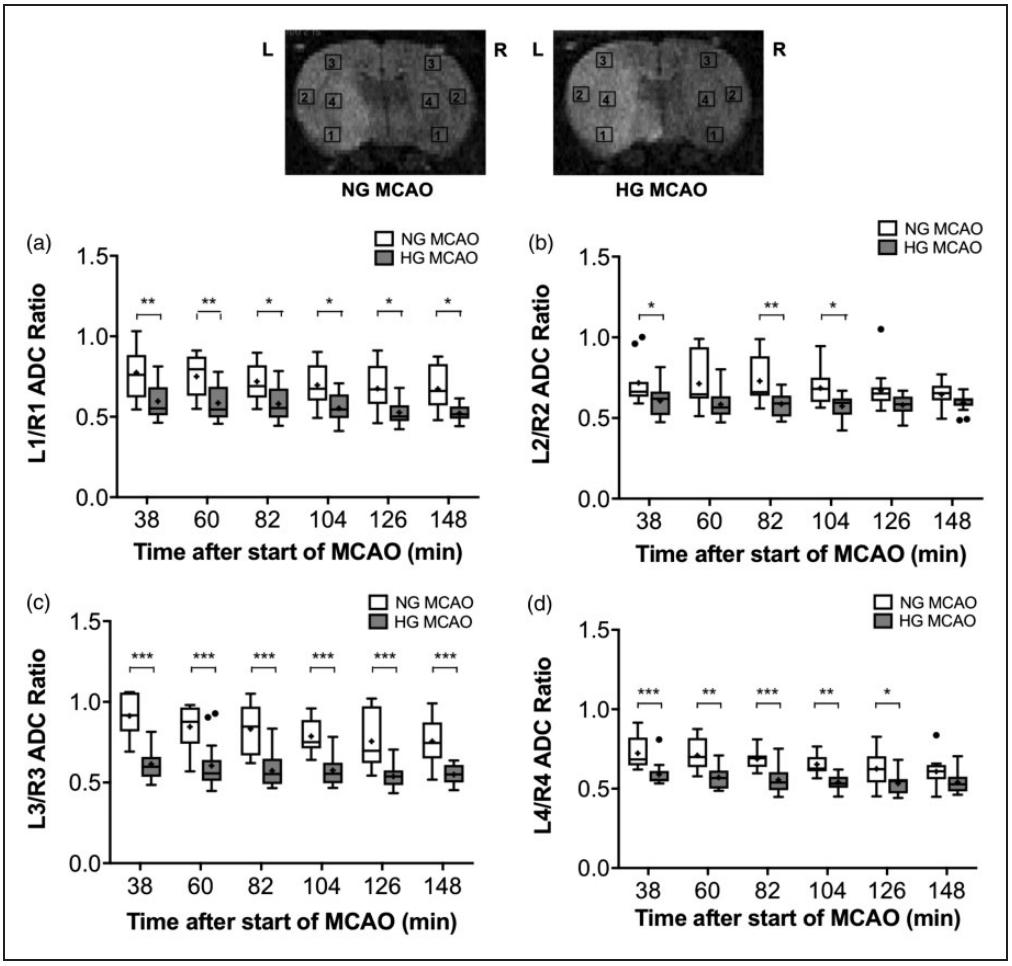

Figure 3. Increased edema formation during MCAO in hyperglycemic rats. Rats made hyperglycemic for 48 h and normoglycemic rats were assessed for brain edema following induction of MCAO by MRI DWI apparent diffusion coefficient (ADC) values for brain regions of interest (ROI 1–4) as depicted in (a). Values shown are ratios of left (ipsilateral) to right (contralateral) ADC values for cortical ROIs 1–3 (a–c) and striatal ROI 4 (d). Data are presented as Tukey box and whisker plots as described in Figure 1. For all plots, *n* values are 11 for normoglycemic rats and 14 for normoglycemic rats. $^{*}p < 0.05$, $^{**}p < 0.0005$, $^{***}p < 0.0001$ compared to control by ANOVA with Bonferroni's multiple comparisons test.

NHE1. BBB endothelial cells possess both NHE1 and NHE2 forms of NHE,[6] and thus we also evaluated high glucose effects on CMEC NHE2 abundance. Neither high glucose exposure nor osmotic control media altered NHE2 abundance (Figure 1(c)). We also conducted qRT-PCR analyses and found that high glucose treatment did not alter NKCC1 mRNA but did cause a transient increase in NHE1 mRNA that was statistically significant only after 24-h exposure (Figure 1(d)). Osmotic control media were without effect.

We next evaluated the effects of high glucose exposure on NKCC and NHE activities (Figure 2(a) to (d)). CMEC NKCC activity was significantly increased following 24-h, 48-h and seven-day exposures (46%, 48% and 64% increases, respectively) as was NHE activity (46%, 48% and 64% increases, respectively) compared to cells exposed to normoglycemic control media.

Hyperglycemia elevates ischemia-induced activity of NKCC and NHE

Our hypothesis predicts that ischemic factors will cause greater increases in NKCC and NHE activities of BBB endothelial cells pre-exposed to hyperglycemic conditions compared to cells maintained in normoglycemic conditions. Figure 2(c) to (d) shows that CMEC exposed for 48 h to high glucose media and then additionally subjected to 60 minutes of hypoxia, aglycemia or AVP had significantly greater NKCC and NHE activities than CMEC exposed to the ischemic factors following 48 h of normal glucose medium. CMEC

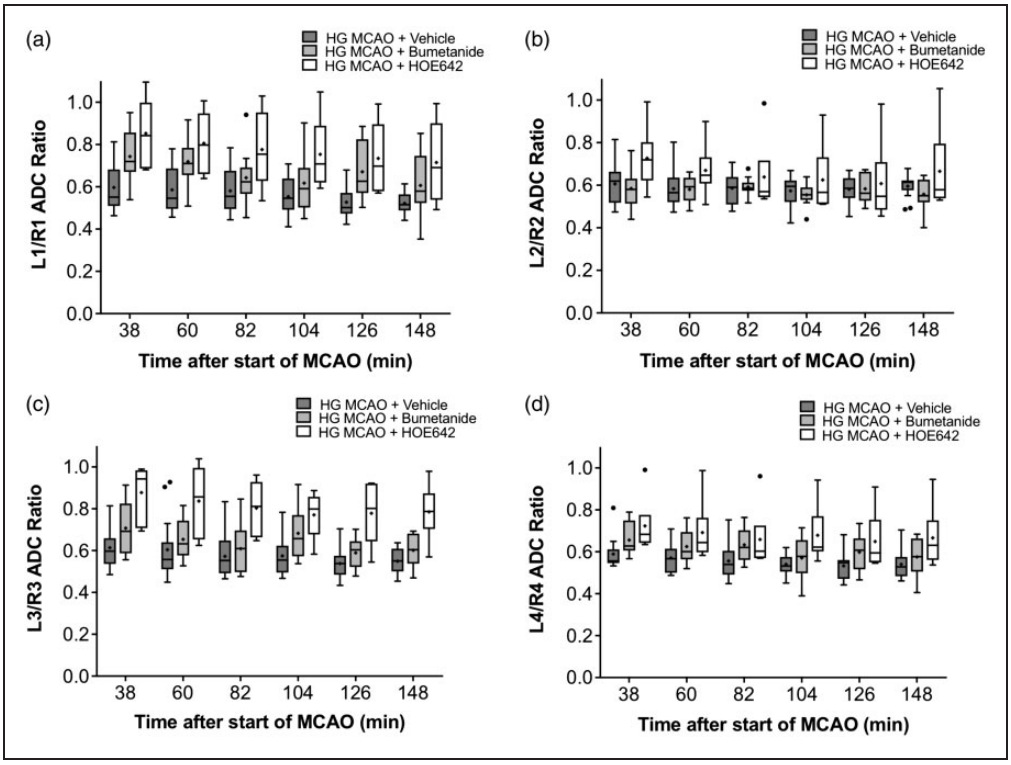

Figure 4. Hyperglycemia-exacerbated edema formation during MCAO is attenuated by bumetanide and HOE-642. Rats made hyperglycemic for 48 h were given vehicle, bumetanide (30 mg/kg) or HOE-642 (15 mg/kg) intravenously immediately before induction of MCAO. ADC ratios are shown for cortical ROIs 1–3 (a–c) and striatal ROI 4 (d). Data are presented as Tukey box and whisker plots as described in Figure 1. For all plots, *n* values are 14, 10 and 6 for vehicle, bumetanide and HOE642, respectively. For statistical analysis, ADC ratios were log-transformed and evaluated in Stata Version 14 using mixed-effects regression models that expressed the mean of the log-transformed ratios (equivalently, the log of the geometric mean ratio) as a function of time and group. Pairwise contrasts between groups were used for hypothesis testing, with contrasts back-transformed and thus expressed as adjusted between-group geometric mean (GM) within-animal (left:right hemisphere) Na ratios with robust 95% CI. One is excluded from the 95% CI when and only when $p < 0.05$. The best fitting model by the Akaike information criteria is a parallel slopes model (in the log-transformed outcome), with random intercepts for animals to capture within-animal correlations among longitudinal measurements. For ADC ratios, geometric mean ratios (GMR) were: L1/R1 bumetanide vs. vehicle GMR (95% CI): 1.18 (1.04, 1.33); L1/R1 HOE642 vs. vehicle GMR (95% CI): 1.36 (1.13, 1.64); L2/R2 bumetanide vs. vehicle GMR (95% CI): 0.99 (0.89, 1.10);L2/R2 HOE642 vs. vehicle GMR (95% CI): 1.15 (0.98,1.35); L3/R3 bumetanide vs. vehicle GMR (95% CI): 1.12 (0.99, 1.28); L3/R3 HOE642 vs. vehicle GMR (95% CI): 1.41 (1.20, 1.65); L4/R4 bumetanide vs. vehicle GMR (95% CI): 1.10 (1.01, 1.19); and L4/R4 HOE642 vs. vehicle GMR (95% CI): 1.21 (1.05, 1.4).

exposed to both high glucose and ischemic factors showed NKCC activity increases of 115%, 69% and 106% and NHE activity increases of 102%, 92% and 140% for hypoxia, aglycemia and AVP, respectively, over that of normoglycemic control cells without ischemic factors.

Intravenous bumetanide and HOE-642 reduce hyperglycemia exacerbation of cerebral edema, brain Na uptake and ischemic injury in rat MCAO

In order to first establish that hyperglycemia exacerbates cerebral edema formation in our rat MCAO model of ischemic stroke as has been reported previously for human hyperglycemic stroke patients,[11,12,16] we subjected rats made hyperglycemic for 48 h to pMCAO and then evaluated cerebral edema formation by MR DWI. We found that hyperglycemia significantly increased cerebral edema formation as indicated by more greatly reduced ADC ratios compared to normoglycemic rats (Figure 3(a) to (d)). As an additional normoglycemic control, we evaluated edema in rats administered STZ and 24 h later given insulin daily to maintain normoglycemia as described in Methods and in Supplementary Information. We found no significant differences in MCAO-induced edema between STZ-insulin normoglycemic rats and normoglycemic rats (non-STZ). Blood glucose levels

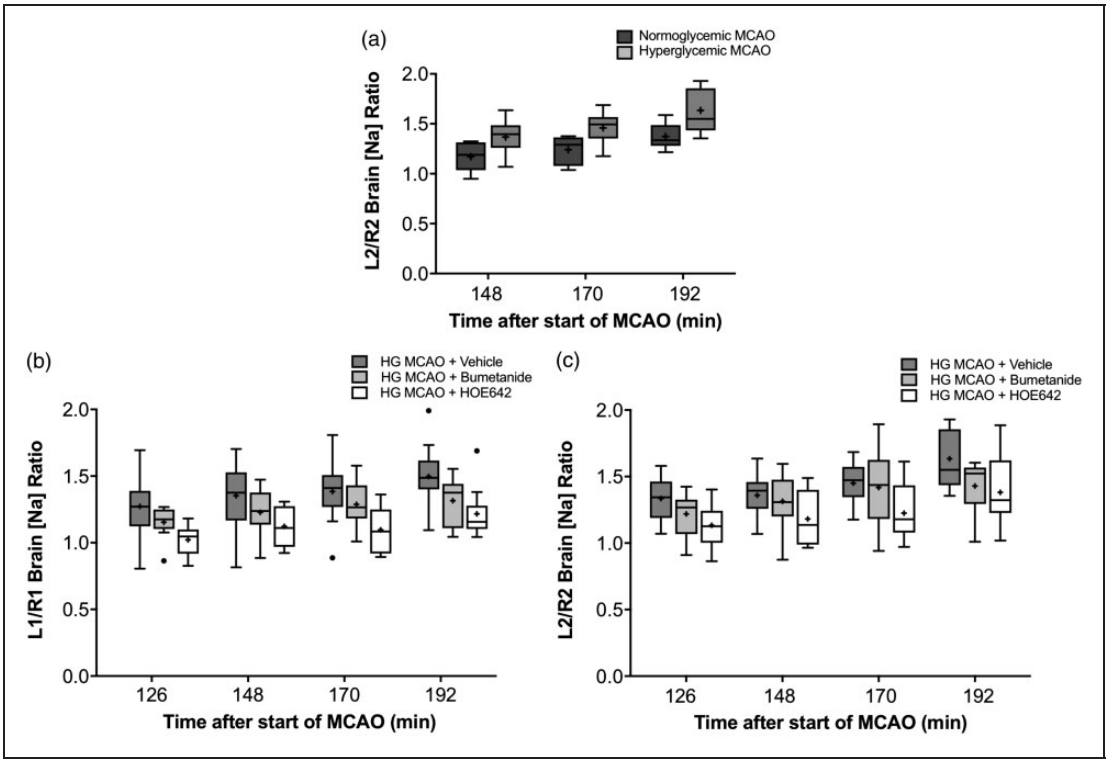

Figure 5. Intravenous bumetanide and HOE-642 attenuate hyperglycemia-elevated brain Na uptake during MCAO. (a) Rats made hyperglycemic for 48 h and normoglycemic rats were subjected to MCAO and then assessed for brain Na uptake by localized 23Na chemical shift imaging (CSI) magnetic resonance spectroscopy (MRS) as described in Materials and Methods. Values shown are ratios of left (ipsilateral) to right (contralateral) [Na] for cortical ROI 2. Data are presented as Tukey box and whisker plots as described in Figure 1. For all plots, *n* values are 6 and 16 for normoglycemic and hyperglycemic rats, respectively. (b,c) Rats made hyperglycemic for 48 h were given vehicle, bumetanide (30 mg/kg) or HOE-642 (15 mg/kg) intravenously immediately before induction of MCAO and then brain [Na] ratios assessed by Na CSI as in (a). Values shown are ratios of left (ipsilateral) to right (contralateral) [Na] for cortical ROIs 1 (b) and 2 (c). Data are presented as Tukey box and whisker plots as described in Figure 1. For all plots, *n* values are 16, 10 and 10 for vehicle, bumetanide and HOE642, respectively. For statistical analysis (a–c), brain Na ratios were log-transformed and evaluated in Stata Version 14 using mixed-effects regression models as described in Figure 4. For Figure 5(a), holding time since the start of MCAO constant, the hyperglycemia vs. normoglycemia adjusted geometric mean ratio (GMR) of L/R brain Na ratios is 1.18 (95% CI: 1.08, 1.28), indicating that hyperglycemia could plausibly increase the typical Na ratio anywhere from 8 to 28% in the population. Geometric mean ratios (GMR) for brain Na data in B and C were: L1/R1 bumetanide vs. vehicle GMR (95% CI): 0.90 (0.82, 0.98); L1/R1 HOE642 vs. vehicle GMR (95% CI): 0.80 (0.74, 0.87); L2/R2 bumetanide vs. vehicle GMR (95% CI): 0.96 (0.89, 1.04); L2/R2 HOE642 vs. vehicle GMR (95% CI): 0.85 (0.77, 0.93).

for the rats in this additional study were 6.6 ± 2.9 and 6.7 ± 0.2 mmol/L (mean $\pm$ SD) for NG vehicle and NG STZ-insulin rats, respectively.

Our previous studies have demonstrated that inhibiting BBB NKCC and NHE by intravenous administration of bumetanide and HOE-642 significantly attenuates ischemia-induced edema and brain Na uptake in normoglycemic rat pMCAO.[1,2] This, together with the observation that hyperglycemia heightens ischemic factor stimulation of BBB NKCC and NHE activities as well as exacerbates ischemia-induced edema formation, suggests that bumetanide and HOE-642 should be an effective means of reducing edema in hyperglycemic ischemic stroke. To test this, rats made hyperglycemic for 48 h were subjected to pMCAO immediately following intravenous administration of bumetanide or HOE-642 and then edema evaluated by DWI. We found that both bumetanide (30 mg/kg) and HOE-642 (15 mg/kg) significantly reduced edema formation (Figure 4). Bumetanide attenuated the drop in cortical ADC ratios by 24% and 12% at 38 and 148 min, respectively, for ROI1 and by 36% and 18% at 38 and 148 min, respectively, for ROI 3 (Figure 4(a) and (c)). HOE-642 also significantly attenuated the drop in ADC ratios by 63% and 40% at 38 and 148 min, respectively, for ROI 1 and by 68% and 52% at 38 and 148 min, respectively, for ROI 3. For striatal ROI 4 (Figure 4(d)), HOE-642 significantly

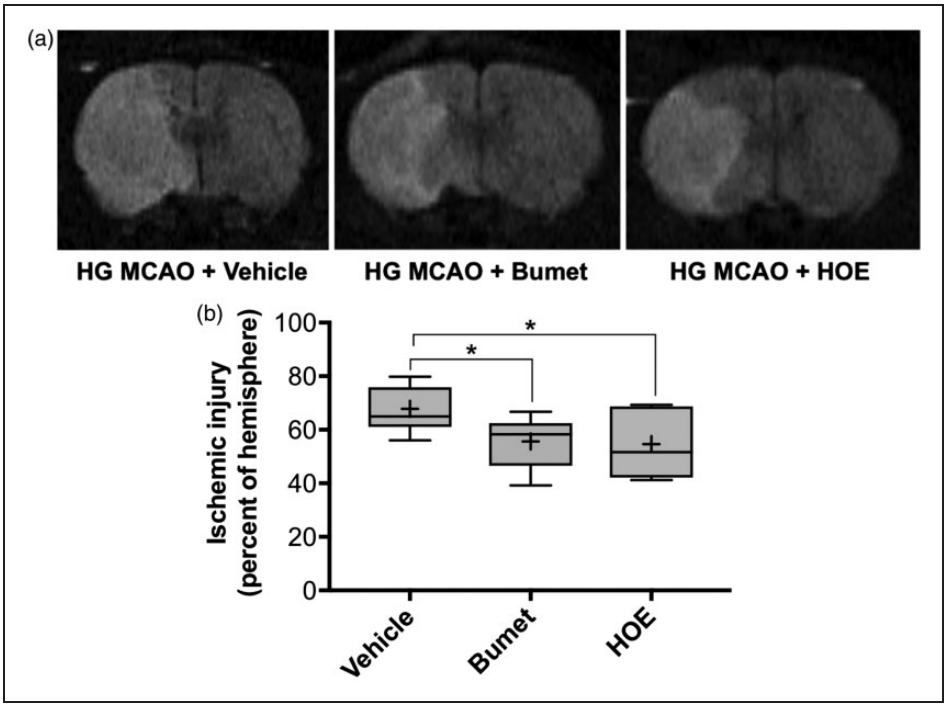

Figure 6. Bumetanide and HOE-642 reduce brain acute ischemic injury in hyperglycemic rats. (a) Representative DWI images from hyperglycemic rats treated with vehicle, bumetanide or HOE-642. Images shown are from B990 scans acquired 170 min after the start of MCAO. (b) Quantitation of acute ischemia area. Data are presented as Tukey box and whisker plots with *n* values of 11, 10 and 5 for vehicle, bumetanide and HOE642, respectively. The DWI B990-defined ischemic injury in hyperglycemic rats treated with bumetanide or HOE-642 is significantly different than hyperglycemic rats treated with Vehicle by ANOVA with Bonferroni's multiple comparisons test, $*p < .05$.

attenuated the drop in ADC ratios, while bumetanide caused a modest reduction that did not reach statistical significance. Neither HOE642 nor bumetanide produced a significant reduction of edema in cortical ROI 2 (Figure 4(b)). No significant differences in physiological parameters, including glucose, plasma electrolytes, hemoglobin or hematocrit, were observed among vehicle- and inhibitor-treated hyperglycemic rat groups (Table 1).

Our previous studies showed that bumetanide and HOE-642 also reduce brain Na uptake in pMCAO,[2] consistent with the assumption that blood to brain secretion of Na is the driving force for ischemia-induced brain water increases.[4] Thus, we also evaluated the effects of bumetanide and HOE-642 on ischemia-induced brain Na uptake in hyperglycemic rats. As predicted, we found that brain Na uptake following induction of pMCAO is increased in the hyperglycemic rats compared to normoglycemic rats (Figure 5(a)). Further, we also found that bumetanide and HOE-642 significantly attenuate the elevated brain Na uptake observed in hyperglycemic rats. Rats treated with HOE-642 showed significantly lower brain Na uptake compared to controls in both ROIs 1 and 2 (Figure 5(b) and (c)). Rats treated with bumetanide showed significantly lower brain Na uptake compared to controls in ROI 1. Bumetanide caused a moderate decrease brain Na uptake in ROI 2 that did not reach statistical significance.

As a further evaluation of intravenous bumetanide and HOE-642 therapeutic potential in hyperglycemic stroke, we used our DWI image data to assess ischemic injury in brains of hyperglycemic rats subjected to MCAO and treated with bumetanide, HOE-642 or vehicle (Figure 6). For this, we determined the area of hyperintensity at B990 as described previously[32] and in Methods. We found that both bumetanide and HOE-642 significantly reduced the extent of injury (B990 abnormality) with 18.0% and 19.4% reductions in bumetanide- and HOE-642-treated rats, respectively. In these studies, we also evaluated the effects of bumetanide and HOE-642 on the volume of cerebral tissue showing compromised mitochondrial function at 170 min of pMCAO by assessing reduced TTC staining. Here, we found that, consistent with previous reports, TTC staining in the early hours of MCAO underestimates the extent of brain injury that evolves by 24 h (Figure 6 Supplement).[34]

Table 1. Physiological parameters of diabetic rats subjected to MCAO.

	(8) NG + Vehicle	(13) HG + Vehicle	(10) HG + Bumet	(6) HG + HOE
Glucose (mmol/L)	9.9 ± 1.6	36.8 ± 3.9***	37.7 ± 2.0***	36.5 ± 5.9***
pH	7.34 ± 0.03	7.29 ± 0.07	7.20 ± 0.22	7.23 ± 0.12
pCO_2 (mm Hg)	39.2 ± 3.7	34.1 ± 6.1	30.4 ± 8.2	42.7 ± 15.4
HCO_3^- (mmol/L)	21.0 ± 1.5	16.3 ± 4.0	13.1 ± 6.6	17.3 ± 4.2
Na^+ (mmol/L)	139.8 ± 2.0	134.0 ± 4.0*	134.4 ± 3.5**	130.8 ± 6.6**
K^+ (mmol/L)	4.5 ± 0.6	5.4 ± 1.1	5.3 ± 1.3	6.0 ± 1.0
Cl^- (mmol/L)	109.4 ± 2.5	104.7 ± 4.3	105.9 ± 4.4	101.2 ± 7.4
BUN (mmol/L)	6.5 ± 1.5	10.9 ± 3.8*	12.9 ± 2.3***	14.6 ± 3.9***
Hemoglobin (g/dL)	12.1 ± 0.9	11.5 ± 1.4	10.6 ± 1.3	11.2 ± 1.2
Hematocrit (PCV decimal fraction)	0.36 ± 0.03	0.34 ± 0.04	0.31 ± 0.03	0.33 ± 0.05

Note: Normoglycemic and hyperglycemic rats were administered bumetanide, HOE-642 or vehicle immediately before induction of MCAO as described in Methods. Values are means ± SD of the number of rats for each group shown in parentheses. *$p < 0.05$, **$p < 0.005$, ***$p < 0.0001$ compared to NG + Vehicle. There are no significant differences among HG groups for any parameter by ANOVA with Bonferroni's multiple comparison test.
MCAO: middle cerebral artery occlusion.

Discussion

The findings of this study support the hypothesis that hyperglycemia exacerbates edema formation in ischemic stroke in part by increasing expression and activity of BBB Na–K–Cl cotransport and Na/H exchange. We show here for the first time that exposing CMEC to high glucose for 24 or more hours increases abundance and activity of both NKCC and NHE and that this increase results in a more exaggerated response to stimulation by ischemic factors than in normoglycemic CMEC. We also show that, in keeping with clinical observations, hyperglycemic rats exhibit exacerbated ischemia-induced edema and brain Na uptake compared to normoglycemic rats. Finally, our findings suggest that BBB NKCC and NHE provide effective therapeutic targets for reducing edema, brain Na uptake and ischemic injury in hyperglycemic stroke.

The present results reveal that hyperglycemic conditions significantly increase abundance of CMEC NKCC1 and NHE1 protein after one-, two- and seven-day exposures. Whether this is true for more chronic exposures of two weeks and beyond remains to be tested. These protein increases are accompanied by elevated NKCC and NHE activities, suggesting that newly expressed Na transporter proteins are present and functional in the plasma membrane. A few previous studies have examined hyperglycemia effects on NKCC and NHE in other vascular tissues. Increased NKCC activity was found in rat aorta and rat mesenteric arteries following two weeks and eight days of STZ-induced diabetes, respectively,[20,35] while NHE expression and activity of human umbilical endothelial cells were reduced following one week of high glucose exposure.[36] In brain studies, choroid plexus cells of hyperglycemic rats show increased NKCC expression but decreased NHE expression.[19] It is possible that the response of NHE to high glucose varies more with cell and tissue type than does that of NKCC. The finding that both NKCC and NHE increase with hyperglycemia in BBB endothelial cells is consistent with both Na transporters participating in heightened ischemia-induced edema during diabetic stroke.

The effect of high glucose on NKCC and NHE activities is unlikely due to an osmotic effect since mannitol and NaCl osmotic controls were without effect. Although hyperosmolarity-induced cell shrinkage rapidly stimulates NKCC and/or NHE activities in many cells, including BBB endothelial cells, to restore intracellular volume through a regulatory volume increase (RVI) response, the RVI is generally complete within an hour at which time the transporter activities return to basal levels.[24,37]

Our previous studies have shown that both NHE1 and NHE2 are present in the luminal BBB membrane in situ.[2,6] The present findings show that hyperglycemic conditions increase NHE1 but not NHE2 protein in these cells. We do not yet know, however, the relative contributions of NHE1 and NHE2 to BBB NHE activity under normoglycemic or hyperglycemic conditions. This is because HOE-642 can inhibit NHE2 in addition to NHE1 activity. Although hyperglycemia does not increase NHE2 abundance, it is still possible that it increases NHE2 activity. Whether there is any NHE2 contribution to the hyperglycemia-induced increase in BBB NHE activity awaits further investigation.

Our hypothesis predicts that hyperglycemia exacerbates edema by ''priming'' the system through

increasing abundance of BBB NKCC and NHE such that subsequent exposure to ischemic factors results in an exaggerated stimulatory response and hypersecretion of Na, Cl and water into the brain. Our present findings demonstrate that exposure to hyperglycemic conditions pre-disposes BBB endothelial cells to a more robust ischemic factor stimulation of NKCC and NHE activities than occurs in normoglycemic cells, whether the ischemic factor is hypoxia, aglycemia or AVP. This is consistent with findings in human hyperglycemic stroke that edema in cerebral ischemia is more pronounced than in non-diabetic stroke patients.[11,12,16]

Our rat model of hyperglycemic stroke mimics the exacerbated edema formation observed in human hyperglycemic patients during ischemic stroke compared to normoglycemic stroke patients. In this regard, rats with 48 hr of STZ-induced hyperglycemia showed significantly greater cytotoxic edema (reduced ADC ratios) compared to normoglycemic rats. This held true for both cortical and striatal ROIs evaluated over the entire imaging period. Our previous studies showed that inhibiting BBB NKCC and NHE activities by intravenous bumetanide and HOE-642, respectively, significantly attenuates edema, brain Na uptake and the TTC-defined volume of ischemia-compromised mitochondrial function (referred to as TTC-defined infarct in those studies) in normoglycemic rats. However, it was unknown whether targeting these BBB Na transporters could effectively reduce edema and injury in the setting of hyperglycemia. Here we show for the first time that bumetanide and HOE-642 do indeed significantly attenuate ischemia-induced cerebral edema in hyperglycemic rats. Both inhibitors also significantly attenuate ischemia-induced brain Na uptake and ischemic injury. Thus, it appears that NKCC and NHE are indeed promising therapeutic targets for hyperglycemic stroke as they are for normoglycemic stroke. A limitation of the present study is that ischemic injury assessed by our DWI scans was determined from one coronal section. It is possible that bumetanide and HOE-642 may affect the extent of injury differently in other brain sections. This will need to be examined in future studies as will long-term outcomes beyond the 170 imaging period of this study. In addition, future studies are needed to determine whether these inhibitors effectively reduce edema in rats made hyperglycemic for different lengths of time prior to ischemia, as well as rats subjected to sustained versus intermittent repeated exposures as occurs in poorly controlled diabetes. Finally, the present studies, both in vitro and in vivo, were purposefully conducted in the absence of insulin in order to determine the effects of high glucose without possible added effects of insulin. This is because insulin as been reported to stimulate NKCC activity in human fibroblasts and skeletal muscle cells.[21–23] It also stimulates NHE activity in hepatocytes but inhibits NHE activity in large artery endothelial cells.[23,28] Future studies will need to clarify the effects of insulin on NKCC and NHE activities of BBB endothelial cells both alone and in the presence of hyperglycemia. A variety of co-morbidities are generally present in diabetics, including hypo- or hyper-insulinemia, hyperlipidemia and inflammatory cytokines. Evaluating the effects of these factors on BBB NKCC and NHE, with their consequent effects on cerebral edema, will necessarily be addressed in future studies.

Several protein kinase pathways have been implicated in cellular responses to high glucose. Two promising candidate pathways are those involving serum- and glucocorticoid-like kinase 1 (SGK-1) and protein kinase C-β (PKCβ). Previous studies have shown that SGK-1 expression and activation are increased by hyperglycemia and that SGK-1 activates a variety of ion channels and ion transporters, including NKCC and NHE.[38] Other studies have found that hyperglycemia activates PKCβ and that PKCβ increases endothelial NKCC activity.[39,40] In ongoing studies we are investigating whether SGK-1 and/or PKCβ participate in the hyperglycemia-induced increases in BBB NKCC1 and NHE1 abundance and activity.

It is not clear whether hyperglycemia-induced increases in NKCC1 and NHE1 resulting in greater ischemia-induced activity of the transporters might represent an adaptive advantage. Indeed, it has yet to be determined why these BBB Na transporters are stimulated to increase secretion of ions and water into the brain during ischemia. One might speculate, however, that when an ischemic focus is quite small, increased secretion of ions and water from blood into brain could provide the advantage of reducing excitotoxicity by flushing neuron-released glutamate out of the ischemic area. If the area of ischemia is large, as occurs in many strokes, it is likely that this increased ion and water secretion is no longer helpful given that the fluid must traverse a greater distance through a more tortuous extracellular space and, instead of providing an effective flushing of glutamate, secretion only adds to the problem as ions and water are rapidly taken up by astrocytes, causing cytotoxic edema (cell swelling) with reduced extracellular space and thus less effective flushing of glutamate. In the case of hyperglycemia with increased secretion of ions and water into the brain, one might predict that astrocyte swelling and increased tortuosity of extracellular space would only occur more rapidly.

A limitation of the present study is that the STZ model of hyperglycemia used produces blood glucose levels significantly higher than detected in most stroke patients. In our model, which maintains rats on insulin post-STZ for several days before insulin withdrawal for 48 h, resulting blood glucose levels are typically

550 mg/dl (30 mM) and higher. Future studies are needed to evaluate the effects of mild to moderate hyperglycemia on BBB processes underlying ischemia-induced cerebral edema. It is noteworthy, however, that in ongoing studies we have found that lower levels of hyperglycemia (10 and 20 mM) also significantly increase CMEC NKCC1 and NHE1 abundance.

In summary, the results of the present study demonstrate for the first time that BBB endothelial cells exposed to hyperglycemic conditions exhibit increased NKCC and NHE protein abundance and activity, along with a significantly heightened response to stimulation by ischemic factors. Consistent with the hypothesis that BBB NKCC and NHE contribute to exacerbated edema formation in hyperglycemic ischemic stroke, we also show here for the first time that inhibiting BBB NKCC and NHE by intravenous bumetanide and HOE-642 significantly reduces edema, brain Na uptake and ischemic injury in hyperglycemic rats subjected to cerebral ischemia. Many potential stroke therapies are thwarted by an inability to reach their targets. As luminal BBB membrane transporters, BBB NKCC and NHE are readily accessible to inhibition by intravenous bumetanide and HOE-642, this, together with our present findings, suggests that BBB NKCC and NHE are promising therapeutic targets for ischemic stroke in hyperglycemic patients.

Funding

The author(s) disclosed receipt of the following financial support for the research, authorship, and/or publication of this article: This work was supported by National Institutes of Health (NIH) R01 NS039953 (MEO), American Diabetes Association grant 1-13-BS-135 (MEO), a University of California, Davis, Clinical Translational Science Center T32 Predoctoral Clinical Research Traineeship (NYY) and a University of California, Davis, Dissertation Year Fellowship (NYY). The studies were conducted in part in a facility constructed with support from National Center for Research Resources Research Facilities Improvement Program Grant C06 RR-17348-01. Funding for magnetic resonance equipment was provided in part by NIH grant RR02511 and by National Science Foundation grant OSTI 97-24412.

Declaration of conflicting interests

The author(s) declared no potential conflicts of interest with respect to the research, authorship, and/or publication of this article.

Authors' contributions

NY Yuen and OV Chechneva contributed equally to the manuscript, performing in vitro experiments, analyzing data and writing parts of the manuscript; Y-J Chen, Y-C Tsai, LK Little and J Dang all performed in vivo experiments, including MCAO surgeries, NMR imaging and data analysis; SE Anderson and J Conston contributed to analysis of NMR data; DJ Tancredi assisted with statistical analyses and ME O'Donnell analyzed in vitro and in vivo data and contributed to the writing the manuscript.

Supplementary material

Supplementary material for this paper can be found at the journal website: http://journals.sagepub.com/home/jcb

References

1. O'Donnell ME, Tran L, Lam T, et al. Bumetanide inhibition of the blood-brain barrier Na-K-Cl cotransporter reduces edema formation in the rat middle cerebral artery occlusion model of stroke. *J Cereb Blood Flow Metab* 2004; 24: 1046–1056.
2. O'Donnell ME, Chen Y-J, Lam TI, et al. Intravenous HOE-642 reduces brain edema and Na uptake in the rat permanent middle cerebral artery occlusion model of stroke: evidence for participation of the blood-brain barrier Na/H exchanger. *J Cereb Blood Flow Metab* 2013; 33: 225–234.
3. Menzies SA, Betz AL and Hoff JT. Contributions of ions and albumin to the formation and resolution of ischemic brain edema. *J Neurosurg* 1993; 78: 257–266.
4. Schielke GP, Moises HC and Betz AL. Blood to brain sodium transport and interstitial fluid potassium concentration during focal ischemia in the rat. *J Cereb Blood Flow Metab* 1991; 11: 466–471.
5. Foroutan S, Brillault J, Forbush B, et al. Moderate to severe ischemic conditions increase activity and phosphorylation of the cerebral microvascular endothelial cell Na-K-Cl cotransporter. *Am J Physiol Cell Physiol* 2005; 289: C1492–C1501.
6. Lam TI, Wise PM and O'Donnell ME. Cerebral microvascular endothelial cell Na/H exchange: evidence for the presence of NHE1 and NHE2 isofroms and regulation by arginine vasopressin. *Am J Physiol Cell Physiol* 2009; 297: C278–C289.
7. O'Donnell ME, Duong V, Suvatne S, et al. Arginine vasopressin stimulation of cerebral microvascular endothelial cell Na-K-Cl cotransport activity is V1 receptor- and [Ca]-dependent. *Am J Physiol Cell Physiol* 2005; 289: C283–C292.
8. Wallace BK, Foroutan S and O'Donnell ME. Ischemia-induced stimulation of Na-K-Cl cotransport in cerebral microvascular endothelial cells involves AMP kinase. *Am J Physiol Cell Physiol* 2011; 301: C316–C326.
9. Wallace BK, Jelks KA and O'Donnell ME. Ischemia-induced stimluation of cerebral microvascular endothelial cell Na-K-Cl cotransport involves p38 and JNK MAP kinases. *Am J Physiol Cell Physiol* 2012; 302: C505–C517.
10. Yuen N, Lam TI, Wallace BK, et al. Ischemic factor-induced increases in cerebral microvascular endothelial cell Na/H exchange activity and abuncance: evidence for involvement of ERK1/2 MAP kinase. *Am J Physiol Cell Physiol* 2014; 306: C931–C942.
11. Ergul A, Li W, Elgebaly MM, et al. Hyperglycemia, diabetes and stroke: focus on the cerebrovasculature. *Vasc Pharmacol* 2009; 51: 44–49.

12. Tureyen K, Bowen K, Linag J, et al. Exacerbated brain damage, edema and inflammation in type-2 diabetic mice subjected to focal ischemia. *J Neurochem* 2010; 116: 499–507.
13. Baird TA, Parsons MW, Barber A, et al. The influence of diabetes mellitus and hyperglycaemia on stroke incidence and outcome. *J Clin Neurosci* 2002; 9: 618–626.
14. Berger L and Hakim AM. The association of hyperglycemia with cerebral edema in stroke. *Stroke* 1986; 17: 865–871.
15. Capes SE, Hunt D, Malmberg P, et al. Stress hyperglycemia and prognosis of stroke in nondiabetic and diabetic patients: a systematic overview. *Stroke* 2001; 32: 26–32.
16. Ribo M, Molina CA, Delgado P, et al. Hyperglycemia during ischemia rapidly accelerates brain damage in stroke patients treated with tPA. *J Cereb Blood Flow Metab* 2007; 27: 1616–1622.
17. Williams B and Howard RL. Glucose-induced changes in Na+/H+ antiport actiity and gene expression in cultured bascular smooth muscle cells. *J Clin Invest* 1994; 93: 2623–2631.
18. Ganz MB, Hawkins K and Reilly RF. HIgh glucose induces the activity and expression of Na+/H+ exchange in glomerular mesangial cells. *Am J Physiol Renal Physiol* 2000; 278: F91–F96.
19. Egleton RD, Campos CC, Huber JD, et al. Differential effects of diabetes on rat choroid plexus ion transporters. *Diabetes* 2003; 52: 1496–1501.
20. Michea L, Irribarra V, Goecke IA, et al. Reduced Na-K pump but increased Na-K-2Cl cotransporter in aorta of streptozotocin-induced diabetic rat. *Am J Physiol Heart Circ Physiol* 2001; 280: H851–H858.
21. Longo N. Insulin stimultes the Na^+,K^+-ATPase and the $Na^+/K^+/Cl^-$ cotransporter of human fibroblasts. *Biochim Biophys Acta* 1996; 22: 38–44.
22. Zhao H, Hyde R and Hundal HS. Signalling mechanisms underlying the rapid and additive stimulation of NKCC activity by insulin and hypertonicity in rat L6 skeletal muscle cells. *J Physiol* 2004; 560: 123–136.
23. Schliess F and Häussinger D. Cell hydration and insulin signaling. *Cell Physiol Biochem* 2000; 10: 403–408.
24. O'Donnell ME, Martinez A and Sun D. Cerebral microvascular endothelial cell Na-K-Cl cotransport: regulation by astrocyte-conditioned medium. *Am J Physiol Cell Physiol* 1995; 268: C747–C754.
25. Livak KJ and Schmittgen TD. Analysis of relative gene expression data using real-time quantitative PCR and the 2(-Delta Delta C(T)) method. *Methods* 2001; 25: 402–408.
26. O'Donnell ME. Endothelial cell sodium-potassium-chloride cotransport. Evidence of regulation by Ca^{2+} and protein kinase C. *J Biol Chem* 1991; 266: 11559–11566.
27. Yuen N, Anderson SE, Glaser N, et al. Cerebral blood flow and cerebal edema in rats with diabetic ketoacidosis. *Diabetes* 2008; 57: 2588–2594.
28. Boedtkjer E and Aalkjaer C. Insulin inhibits Na^+/H^+ exchange in vascular smooth muscle and endothelial cells in situ: involvment of H_2O_2 and tyrosine phosphatase SHP-2. *Am J Physiol Heart Circ Physiol* 2009; 296: H247–H255.
29. Moore RD. Effects of insulin upon ion transport. *Biochim Biophys Acta* 1983; 737: 1–49.
30. Sargeant RJ, Liu Z and Klip A. Action of insulin on Na+-K+-ATPase and the Na+-K+-2Cl- cotransporter in #T#-L1 adipocytes. *Am J Physiol Cell Physiol* 1995; 269: C217–C225.
31. O'Donnell ME, Lam TI, Tran LQ, et al. Estradiol reduces activity of the blood-brain barrier Na-K-Cl cotransporter and decreases edema formation in permanent middle cerebral artery occlusion. *J Cereb Blood Flow Metab* 2006; 26: 1234–1249.
32. Campbell BCV and Macrae IM. Translational perspectives on perfusion-diffusion mismatch in ischemic stroke. *Int J Stroke* 2015; 10: 153–162.
33. Lo EH, Pierce AR, Mandeville JB, et al. Neuroprotection with NBZQ in rat focal cerebral ischemia. Effects on ADC probability distribution functions and diffusion-perfusion relationships. *Stroke* 1997; 28: 439–447.
34. Liu F, Schafer DP and McCullough LD. TTC, Fluoro-Jade B and NeuN staining confirm evolving phases of infarction induced by middle cerebral artery occlusion. *J Neurosci Methods* 2009; 179: 1–8.
35. Dilley RJ, Ferrelly CA, Allen TJ, et al. Diabetes induces Na/H exchange activity and hypertrophy of rat mesenteric but not basilar arteries. *Diabetes Res Clinl Pract* 2005; 70: 201–208.
36. Zerbini G, Roth T, Podesta E, et al. Activity and expression of the Na+/H+ exchanger in human endothelial cells cultured in high glucose. *Diabetologia* 1995; 38: 785–791.
37. Pedersen SF, O'Donnell ME, Anderson SE, et al. Physiology and pathophysiology of Na^+/H^+ exchange and Na^+-K^+-$2Cl^-$ cotransporter in the heart, brain and blood. *Am J Physiol Regl Inter Comp Physiol* 2006; 291: R1–R25.
38. Lang F, Görlach A and Vallon V. Targeting SGK1 in diabetes. *Expert Opin Ther Targets* 2009; 13: 1301–1311.
39. Cipolla M, Huang Q and Sweet JG. Inhibition of protein kinase Cβ reverses increased blood-brain barrier permeability during hyperglycemic stroke and prevents edema formation in vivo. *Stroke* 2011; 42: 3252–3257.
40. Yang T, Roger KE, Bhat GJ, et al. Protein kinase C family members as a target for regulation of blood-brain barrier Na,K,2Cl cotransporter during in vitro stroke conditions and nicotine exposure. *Pharm Res* 2006; 23: 291–302.